

10A.5 HAIL DETECTION WITH A C-BAND DUAL POLARIZATION RADAR IN THE CANADIAN GREAT LAKES REGION.

Sudesh Boodoo¹, D. Hudak¹, M. Leduc¹, A. V. Ryzhkov², N. Donaldson¹, and D. Hassan³

(1) King City Weather Radar Research Station, Environment Canada, (2) Cooperative Institute for Mesoscale Meteorological Studies, University of Oklahoma, (3) Pelmorex Media Inc., Canada.

1. INTRODUCTION

Hail detection by conventional Doppler radar is based on volumetric measurements of horizontal radar reflectivity (Z_H). Typically reflectivity derived algorithms such as vertically integrated liquid (VIL) are used since this quantity has been shown to correlate with severe weather (Elevander 1977). Dual polarized radar provides the additional variables, differential reflectivity (Z_{DR}), cross-correlation coefficient (ρ_{HV}), linear depolarization ratio (LDR), and differential phase (Φ_{DP}), (Bringi and Chandrasekar 2001), which are indispensable for classifying and quantifying meteorological targets. Studies by Balakrishnan and Zrnić (1990), Hubert et al. (1998), and Kennedy et al. (2001), have all utilized these variables or a subset thereof to detect hail.

The National Severe Storms Laboratory (NSSL) supported the Joint Polarization Experiment (JPOLE) (Ryzhkov et al. 2005) in 2003 during which polarimetric data in a variety of storm environments were collected. A fuzzy logic hydrometeor classification algorithm (HCA) using Z_H , Z_{DR} , ρ_{HV} and reflectivity texture ($SD(Z)$) was tested. Heinselman and Ryzhkov (2004, 2006) evaluated the hail detection capability of the HCA and compared it to a conventional hail detection algorithm (HDA) based on the storm reflectivity structure, Witt et al. (1998). The HDA algorithm is currently used in the Weather Surveillance Radar-1988 Doppler (WSR-88D) system. They pointed out shortcomings in the HDA such as its reliance on vertical structure of Z_H in the storm cell, the empirically derived factors for converting reflectivity to hail probabilities

and the hail location as being non-specific. It was stated that the HCA outperformed the HAD algorithm and resulted in a probability of detection (POD) of 100% and 88% respectively, for the analyzed dataset. Furthermore the calculated false alarm ratio (FAR) for HCA was much lower at 11% compared to 39% for HDA.

This study parallels the work by Heinselman and Ryzhkov (2004) to assess the quality of the Environment Canada (EC) current hail detection algorithms, with several notable differences. First we employ data collected by dual polarized C-band radar as opposed to the S-band system. This poses a challenge with significant attenuation when investigating severe hail producing storms. Second the volumetric Z_H is collected simultaneously with the polarimetric variables. The verification data used were from observer reports of hail location and time at the ground.

Section 2 overviews the radar characteristics and modes of data collection. Some details about the radar data are also presented. Section 3 describes the algorithms used for hail detection, and notes about the verification data. Section 4 overviews the methodology for assessing the algorithms with the observations. Results of the statistical analysis are presented in section 5 with specific examples of the algorithms output and section 6 provides the summary and conclusions.

2. RADAR CHARACTERISTICS

The King City C-band dual polarimetric scanning Doppler radar (WKR) is located just north of Toronto in southern Ontario, Canada. The antenna diameter is 6.1 m and produces a beam width of 0.62° (Hudak et al. 2006). The radar employs the

Corresponding author address: Sudesh Boodoo, King Weather Radar Research Station, 14780 Jane St. King City, ON, Canada, L7B-1A3.
email: Sudesh.Boodoo@ec.gc.ca

simultaneous transmission and reception of the horizontally and vertically polarized wave, so-called “slant 45” technique. This allows for the collection of Z_{DR} , ρ_{HV} and Φ_{DP} in addition to Z_H . The volumetric data scan (called “CONVOL”) is collected to a range of 250 km in 4 minutes and repeated at 10 minute intervals. The spatial resolution for this dataset is 1km by 1° . The second dual polarimetric data collection mode (called “POLPPI”) is the high spatial resolution data set, 0.25 km by 0.5° , collected out to 112 km at a 0.5° elevation.

3. HAIL DETECTION

a. Hail algorithm of the Canadian Radar Decision System (CARDS)

The CARDS (Joe et al. 1995, Lapczak et al. 1999) is the unified radar data processing software used in the EC radar network. One product of the system is the hail output used by forecasters to issue warnings of occurring severe weather. The hail algorithm (Joe et al. 2004) is empirically based and uses only the volumetric scans of Z_H from the CONVOL product. Estimates of hail size are derived from the maximum height of the 50 dBZ height or the VIL and freezing level. The algorithm output is the larger of the two estimates with its location and extent. Reference to this algorithm will be denoted by “URPHail” throughout the paper. Figure 1 shows an example output from the algorithm at 0300 UTC 2007-Jul-21. The freezing level was at 4.0 km from model data and the maximum hail size was 8.3 cm at range 57 km and azimuth 58° . Many other scattered hail pixels of varying sizes are also seen north of the radar.

b. Interactive Particle Classification Algorithm (“iParCA”)

The iParCA classification algorithm was created as an interactive analysis tool employing fuzzy logic techniques developed by NSSL and adapted for C-Band (Ryzhkov et al. 2007). Processing is done in two stages. In stage 1, the variables Z_H , Z_{DR} , ρ_{HV} , $SD(Z)$ and differential phase texture $SD(\Phi_{DP})$ are used to perform a preliminary classification. The outputs are classes for meteorological scatterers, biological

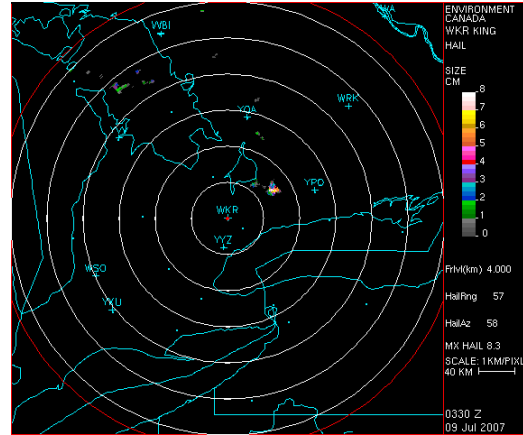


Figure 1. Example output from the “URPHail” algorithm at 0300 UTC 2007-Jul-21. Range rings are 40 km apart.

scatterers, ground clutter and unknown. Since signal attenuation at C-band for both Z_H and Z_{DR} are significant for convective storm cells containing large drops and possibly hail, therefore correction techniques (Ryzhkov et al. 2006, 2007) were applied at this stage. The meteorological class from stage 1 is then combined with Z_H , Z_{DR} , ρ_{HV} , specific differential phase (K_{DP}), velocity (V) and the height of the melting level in stage 2 processing. 1-D and 2-D trapezoidal membership functions are used in the fuzzy logic approach with appropriate weightings to give a final classification of a particular pixel. This results in the 8 hydrometeor classes, dry snow (DS), wet snow (WS), crystals (CR), graupel (GR), big drops (BD), rain (RA), heavy rain (HR) and rain/hail (RH). Table 1 is a subset of the polarimetric parameters with their fuzzy logic ranges for RH pixels utilized in our analysis.

Polarimetric variable	iParCA RH range
Z_H	45-80 dBZ
Z_{DR}	-0.3-1dB
ρ_{HV}	0.75-0.96
Φ_{DP}	Abrupt changes

Table 1. iParCA fuzzy logic ranges on a few of the polarimetric variables used for the rain/hail (RH) classification.

Hydrometeor classification can be performed on both the CONVOL and POLPPI scans. Figure 2 is an example output from the iParCA classification at 0300

UTC 2007-Jul-21 from the 0.5° POLPPI. The purple pixels indicate the RH class, seen to the northeast of the radar, near the 60 km range ring. The two hail cores are clearly seen from this high resolution data. It is noteworthy that the signal is completely lost behind the hail shafts due to extreme attenuation.

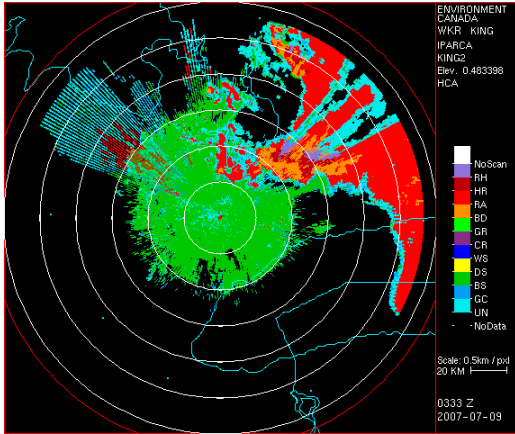


Figure 2. Example output from the iParCA algorithm at 0300 UTC 2007-Jul-21 from the high resolution 0.5° POLPPI scan. Range rings are 20 km apart.

4. METHODOLOGY OVERVIEW

During the summers of 2005-2009, 24 days with severe convective weather potentially producing hail were selected. From these days we have selected 79 storm cells for the dataset comprising of super cells (SC) and multi-cell storms (MC) of varying duration and severity. The cells were located at distances ranging from 6 km to 213 km from the radar.

The iParCA classification algorithm was run for the 79 storm cells on the 0.5° elevation of CONVOL and then again on the 0.5° POLPPI scans. The URPhail CONVOL output was directly compared to the iParCA CONVOL (0.5°) because all the polarimetric variables are collected simultaneously with Z_H . With POLPPI and URPhail comparisons there is about a 5 minute offset between the detections from their respective data scans.

Reports of hail location and time were collected through EC's volunteer weather watcher network and Pelmorex Media Inc. Storm Line. Probability of hail from the NEXRAD hail algorithm from the

Buffalo WSR-88D (KBUF) radar for these storm cells were also used to supplement the verification data.

Contingency table of hits (H) misses (M) and false alarms (FA) were used to compute the skill scores POD, FAR, critical success index (CSI) and BIAS for assessing performance of the algorithms.

5. RESULTS

a. Statistical Performance of the algorithms

The selected 79 storm cells provided the basis for investigating the relative performance of the reflectivity hail detection algorithm with the polarimetric hail algorithm. Table 2 shows that for the total observed cells, iParCA had over 20% more hits and 75% fewer misses than the URPhail algorithm. False alarms were slightly higher with iParCA.

	iParCA	URPhail
H Total	68	55
M Total	4	17
FA Total	5	3

Table 2. Totals of hits (H), misses (M) and false alarms (FA) comprising the total storm cells studied.

The 2x2 contingency matrix of the standard skill scores are provided in table 3. The CSI and POD were better for the polarimetric method of hail detection and are 88% and 94% respectively compared to 73% and 76% for the reflectivity only approach to hail detection. The BIAS score shows that iParCA has a small tendency to over estimate hail detections, but still much better than the large underestimation of the URPhail detection algorithm. FAR were about the same for both algorithms.

	iParCA	URPhail
CSI	88.3	73.3
BIAS	1.4	-19.4
POD	94.4	76.4
FAR	6.8	5.2

Table 3. Standard skill scores measures as percentages for the 79 cells in the dataset.

b. Detail study for a subset of cells

Of the 79 cells in total 35 were selected for detailed investigation to provide insight into the possible physical reasons for the superiority of the polarimetric detections. Stratification of these 35 cells into MC and SC categories resulted in 19 cells classed as multicell storms and 16 as supercell storms. Tables 4 and 5 summarize the skill scores when the detections are treated separately.

MC	iParCA	URPHail
CSI	89.5	63.2
BIAS	11.8	-17.6
POD	100.0	70.6
FAR	10.5	14.3

Table 4. Skill score measures in percentages for the 19 MultiCell (MC) cases.

SC	iParCA	URPHail
CSI	100.0	75.0
BIAS	0.0	-25.0
POD	100.0	75.0
FAR	0.0	0.0

Table 5. Skill score measures in percentages for the 16 SuperCell (SC) cases.

For the MC cases (table 4) iParCA has 100% POD compared to 71% with URPHail. The CSI is close to 90% compared to 63% with URPHail. False alarms were relatively high for both types of hail detection methods in these types of storms. For the 16 SC cases (table 5) iParCA had perfect scores for this data set and suggest that on days with supercell storms, polarimetric hail detection would have the most benefit.

c. Physical reasons for superior polarimetric hail detection

From the 35 cells comprising 13 study days it was found that iParCA subjectively performed better in terms of quality of the information in 23 of the cases. The quality assessment and reasons for iParCA superiority were characterized by 4

groups, with an example given for each group :-

1. Geometry/Timing

This refers to cases where the storm is close to the radar so that only lower portions are scanned. This results in unrealistically low VIL and height of the 50 dBZ level, causing hail detection failure for the URPHail algorithm.

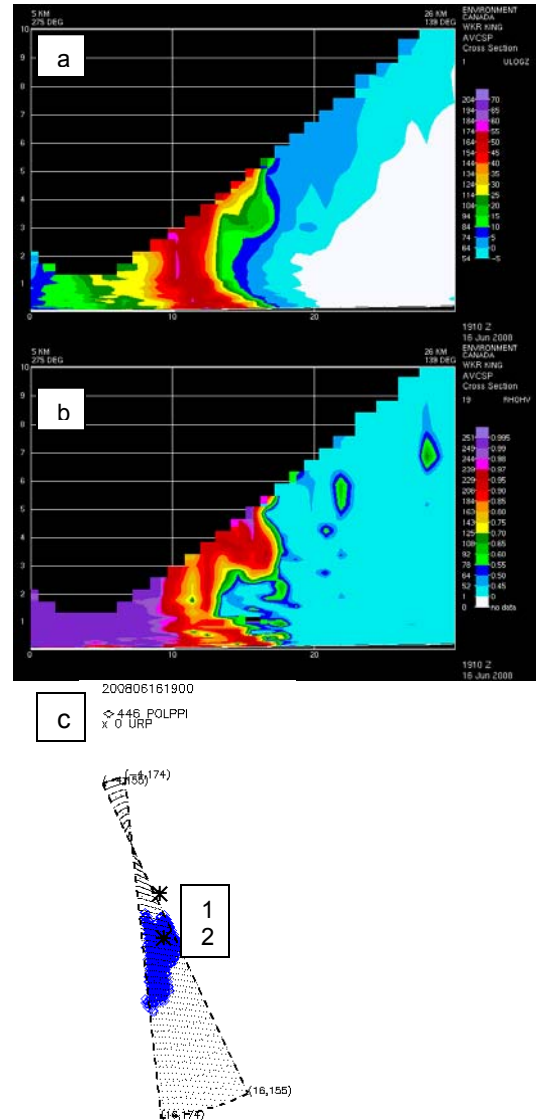


Figure 3. Vertical cross-section of Z_H (a) and ρ_{HV} (b) for a storm cell close to the radar at 1900 UTC 2008-Jun-16. (c) iParCA hail pixels (blue) locations from the 0.5° POLPPI scan. Asterisks 1 and 2 marks specific pixel locations referred to in the text.

Figure 3(a, b) shows the vertical cross-sections of reflectivity and cross-correlation coefficient for a storm cell at 1900 UTC on 2008-Jun-16. Because of the cell close proximity to the radar, the upper level of the storm is not seen and the URPHail algorithm detects no hail. The reflectivity values at the center of the cell close to ground level reach approximately 55 dBZ (fig. 3a), the corresponding region in figure 3b shows low ρ_{HV} in the range 0.7-0.8. The polarimetric classification on the 0.5° POLPPI scan shows the hail pixels (blue) in figure 3c. Asterisk 1, closest to the radar, has corrected horizontal reflectivity (Z_{corr}) of 49.5 dBZ, corrected Z_{DR} of 2.2 dB, and ρ_{HV} of 0.98. Values at asterisk 2 in the hail region were 52.5 dBZ, 0.53 dB and 0.76 respectively for the same polarimetric quantities. This geometry effect was most significant for storm cells within 13 km of the radar. Timing refers to hail being detected in one scan and not the other i.e. hail may be detected in a POLPPI scan but not the corresponding CONVOL. The 5 minutes between the scans may be sufficient for the storm property to trigger the hail detection algorithms. 2 cells form our detailed cases showed the geometry effect while 3 were for the timing reason.

2. Attenuation

Significant path attenuation occurs at C-band during heavy rain fall, thus potentially severe hail producing storms may not be seen adequately by the radar. The following example is the Grimsby hailstorm of 2008-Jul-23. Figure 4a-c shows and enhanced view of Z_{corr} , ρ_{HV} , Φ_{DP} and VIL for this storm at 0140 UTC.

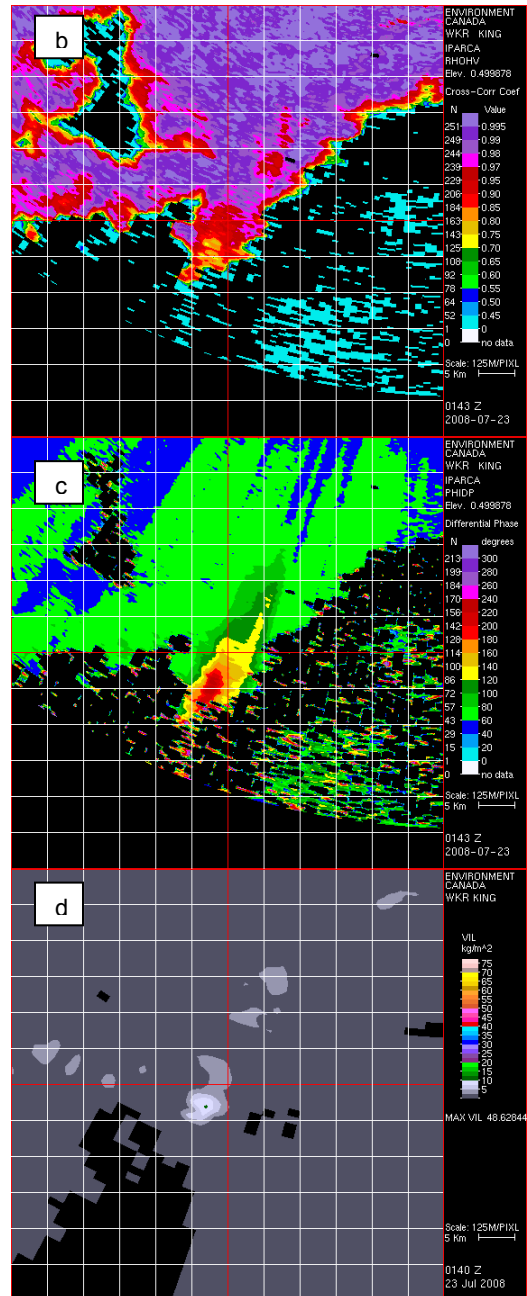
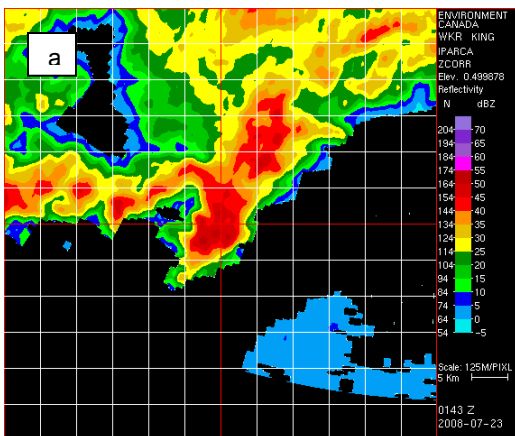


Figure 4. (a) Corrected horizontal reflectivity (Z_{corr}), (b) ρ_{HV} , (c) Φ_{DP} and (d) VIL at 0140 UTC on 2008-Jul-23. Red cross hairs are at 94 km and 201° from the radar.

The “center” of the cell is located at the red crosshairs at 94 km and 201° from the radar. Reflectivity of about 55 dBZ are seen in the cell. Echotop for this cell was around 10 km. Figure 4b shows ρ_{HV} in the cell area. In the rain region closer to the radar it is almost 1.0. At the most intense region of the storm cell ρ_{HV} drops to 0.90 and then to 0.7

towards the rear of the storm. Very abrupt change in Φ_{DP} is seen in figure 4c, with value increasing from 100° to over 220° over a very short range. The VIL was concentrated to a small region shown in figure 4d. The hail pixel location map is shown in figure 5. URPHail fails to find hail in this case at this time. At pixel location 1 (fig. 5) Z_{corr} was 46 dBZ, corrected Z_{DR} was 1.05 dB, and ρ_{HV} was 0.93 with iParCA class HR. For pixel location 2 (R/H class), the values were 50 dBZ, 0.14 dB and 0.82 respectively for Z_{corr} , corrected Z_{DR} and ρ_{HV} . Hail swath of 20 km long with many stones up to 3 cm developed after this time. Polarimetric radar may have been seeing hail which was not detected by attenuated affected URPHail and un-attenuated KBUF (reflectivity of 60 dBZ) hail algorithms. No hail was reported at the ground at this time but was likely aloft. Five of the 35 cases were identified as having better polarimetric detectability over the conventional hail algorithm because of attenuation.

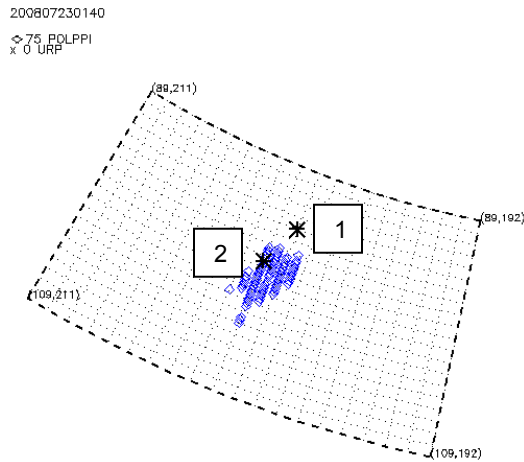


Figure 5. Hail pixel map at 0140 UTC on 2008-Jul-23. Blue pixels showing hail extent from the POLPPI scan. Asterisks 1 and 2 marks specific pixel locations referred to in the text.

3. Dual polarization discrimination

There were 11 situations where iParCA was subjectively better at hail detection. Although URPHail did detect hail, the quality of the information such as hail extent was deemed better using the polarimetric algorithm. The example presented here is at 1740 UTC on 2005-Jun-09. Figure 6a shows the iParCA

classification out for the POLPPI product. Two distinct regions of hail are seen within the storm at 50 km 341° and 53 km 343° from the radar.

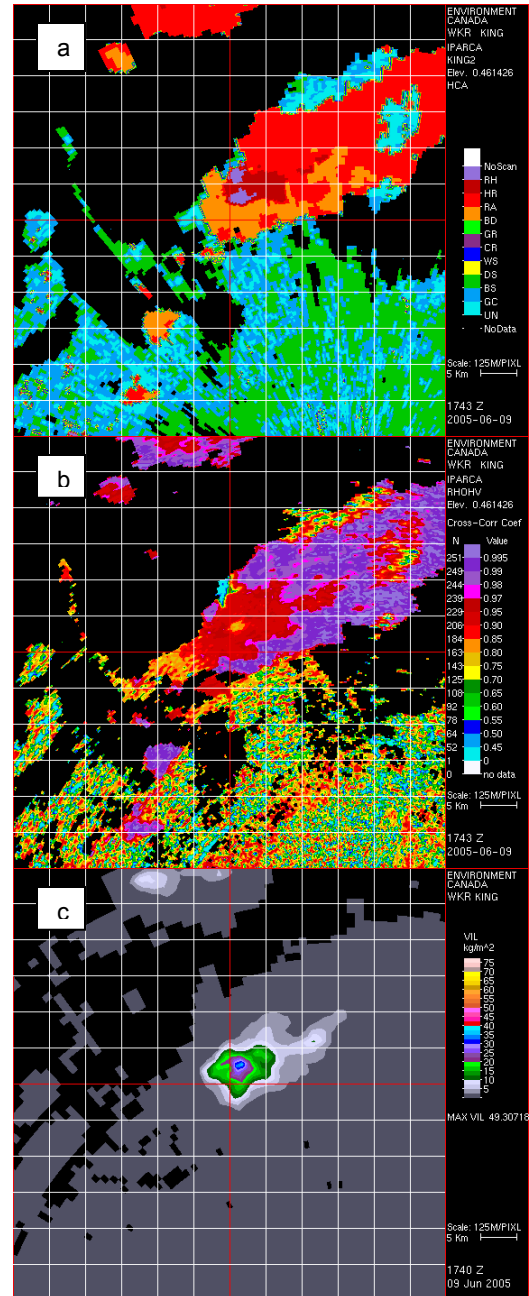


Figure 6. (a) iParCA classification output for storm cell at 1740 UTC 2005-Jun-09. (b) ρ_{HV} (c) VIL. Red crosshairs is at 47 km 339° from the radar.

200506091740
 ◇ 128 POLPPI
 x 26 URPHail

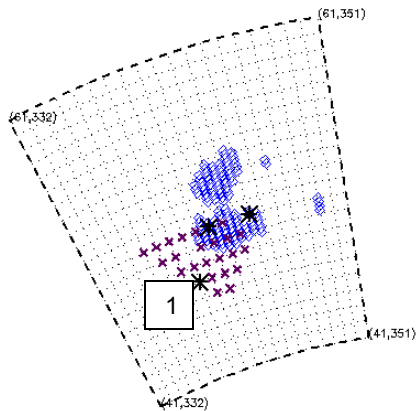


Figure 7. Hail pixel location map showing pixels from URPHail (purple x's) and POLPPI iParCA pixels (blue diamonds). The storm cell at 1740 UTC 2005-Jun-09. Asterisk 1 mark the pixel location referred to in the text.

Figure 6b. shows the ρ_{HV} distribution in the storm cell. For a large part of the storm the value is close to 1.0 with a smaller region having lower ρ_{HV} of 0.75. compared to iParCA, URPHail shows a much larger extent of hail indicated by the strong VIL values in figure 6c. The hail pixels extent is pronounced in figure 7. Values at location 1 in figure 7 are, Z_{corr} of 39 dBZ, Z_{DR} corrected of 4.8 dB and ρ_{HV} of 0.91. This suggests that this part of the URPHail area, confused as hail, is actually heavy rain. The dual polarimetric parameters were better at discriminating the heavy rain region with no hail and rain/hail region.

4. Storm overhang displacement

Supercell storms often have big overhangs. The height of the 50 dBZ level often ends up in the overhang, and VIL will be skewed to this region of the storm. In such situations it is expected that URPHail will overestimate the hail and misplace its location in the overhang. On 2009-May-09 several waves of storm moved across the Greater Toronto Area, with several reports of hail in the 3-5 cm range.

Figure 8a shows the vertical cross-section of reflectivity at 1300 UTC 2009-May-09 showing the large overhang. The storm top is approximately at 8 km. The high

reflectivity (50 dBZ or more) core at 5.0 km is displaced a few kilometers from the decreased ρ_{HV} (0.9) core at the ground in figure 8b. The melting layer can also be seen in figure 8b at about 2.0 km. Z_{DR} of 1.0-2.0 dB is seen just behind the heavy rain region ($Z_{DR} > 2.0$ dB) at the 30 km mark on the horizontal axis in figure 8c.

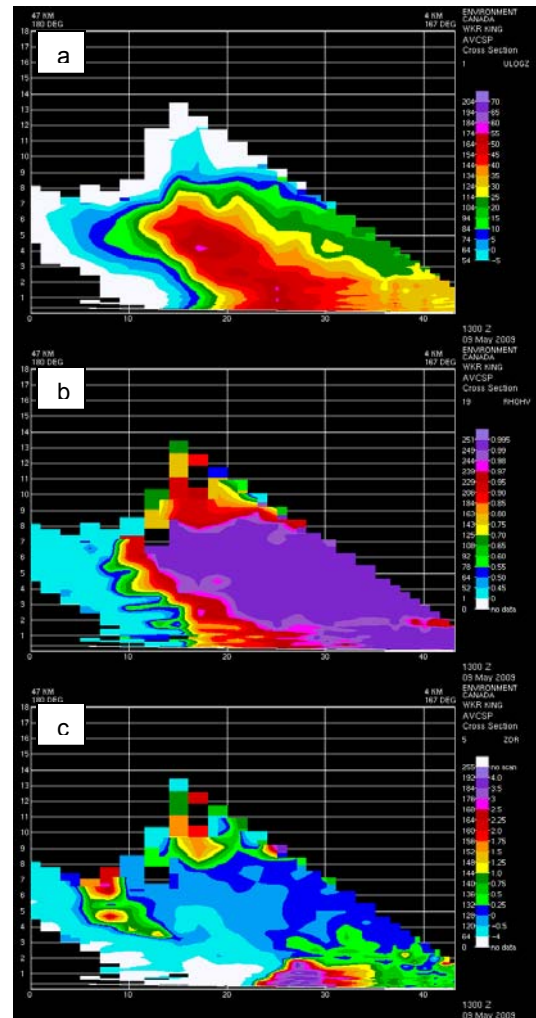


Figure 8. 1300 UTC 2009-May-09 vertical cross-sections of (a) Z_H , (b) ρ_{HV} , and (c) Z_{DR} .

Figure 9 is the hail pixel map of detections from URPHail and iParCA. The URPHail pixels (purple x's) and the iParCA CONVOL (red +s) are from the same radar scan. The URPHail pixels are displaced further to the south (i.e. mostly in the storm top overhang) of the iParCA hail pixels. The observer hail report (yellow star) matches well with the concentration of the iParCA pixels. Displacement between CONVOL and

POLPPI pixels is due to the storm motion during the time difference between the scans. This overhang displacement was seen in 6 of our SC cases.

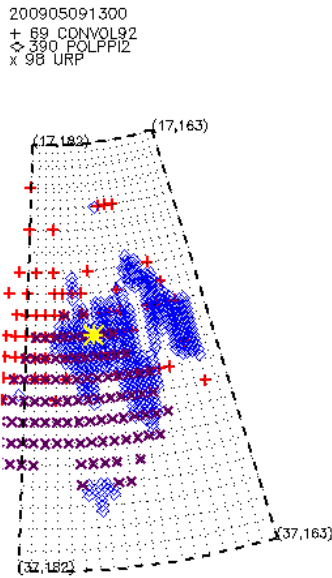


Figure 9. 1300 UTC 2009-May-09 hail pixel locations from iParCA POLPPI(blue diamonds), iParCA CONVOL(red +’s), and URP Hail (purple x’s). Yellow star indicate the location of the observer reports of hail on the ground.

6. SUMMARY AND CONCLUSIONS

Hail detection using C-band dual polarimetric data has been investigated from a data set of 79 storm cell collection from 2005-2009. The hail algorithm based on reflectivity and storm structure (URPHail) was compared to a polarimetric classification algorithm (iParCA). The polarimetric algorithm is based on a fuzzy logic approach using weighted membership functions of Z_H , Z_{DR} , ρ_{HV} , $SD(Z)$ and $SD(\Phi_{DP})$.

The polarimetric method of detection outperformed the reflectivity only method with POD of 94% versus 76%, respectively. CSI was also better at 88% versus 73% in favor of polarimetric hail detection. The FAR was found to be slightly greater in iParCA than URP Hail, but both were still quite low at under 7%.

Subsequent detail analysis of a subset of the data revealed several physical

reasons for the superior polarimetric hail detection method.

- 1) Geometry/Timing:- Storm cell close to radar, so upper levels are not seen causing failure of the URP Hail algorithm. Hail being identified by the polarimetric algorithm on the high spatial resolution scan and not the corresponding low resolution scan due to storm motion.
- 2) Attenuation:- Storms are severely attenuated so that URP Hail thresholds are not met and thus fails to detect hail.
- 3) Dual polarization discrimination:- iParCA showing less hail compared to URP Hail. URP Hail cannot distinguish between heavy rain and hail. Z_{DR} and ρ_{HV} are essential for this.
- 4) Storm overhang misplacement:- URP Hail focuses on the high reflectivity in the upper level of supercell storms, which often have significant overhang.

It was also found that iParCA performs best with supercell storms when compared to multi cellular situations.

Acknowledgements We would like to thank J.M.C. Young for the discussions into the intricacies of the interactive Particle Classification Algorithm.

References

- Balakrishnan, N., and D. S. Zrnić, 1990: Use of polarization to characterize precipitation and discriminate large hail. *J. Atmos. Sci.*, 47,1525-1540.
- Bringi, V. N., and V. Chandrasekar, 2001: *Polarimetric Doppler Weather Radar: Principles and Applications*. Cambridge University Press, 636pp.
- Elevander, R. C., 1977: Relationships between radar parameters observed with objectively defined echoes and reported severe weather occurrences. Preprints, *10th Conf. on Severe Local Storms*, Omaha, NE, Amer. Meteor. Soc., 73-76.

Heinselman, P.L., and A. V. Ryzhkov, 2004: Hail detection during the Joint Polarization Experiment. Preprints, *22nd Conf. on Severe Local Storms*, Hyannis, MA, Amer. Meteor. Soc., http://ams.confex.com/ams/11aram22sls/techprogram/paper_81148.htm73-76.

----, and A. V. Ryzhkov, 2006: Validation of Polarimetric Hail Detection. *Wea. And Forecasting*, 21, 839-850.

Hubbert, J., V. N. Bringi, L. D. Carey, and S. Bolen, 1998: CSU-CHILL polarimetric radar measurements from a severe hail storm in eastern Colorado. *J. Appl. Meteor.*, 37, 749-775.

Hudak, D., P. Rodriguez, G. W. Lee, A. V. Ryzhkov, F. Fabry, and N. Donaldson, 2006: Winter Precipitation Studies with a Dual Polarized C-band Radar. Preprints, *Fourth European Conf. on Radar in Meteorology and Hydrology (ERAD 2006)*, Barcelona, Spain, 9-12.

Joe P., Coauthors, 1995: Recent progress in the operational forecasting of summer severe weather. *Atmos.-Ocean*, 33, 249-302.

----, D. Burgess, R. Potts, T. Keenan, G. Stumpf, and A. Treloar, 2004: The S2K Severe Weather Detection Algorithm and Their Performance. *Wea. And Forecasting*, 19, 43-63.

Lapczak S., Coauthors, 1999: The Canadian National Radar Project. Preprints, *29th Int. Conf. on Radar Meteorology*, Montreal, QC, Canada, Amer. Meteor. Soc., 327-330.

Kennedy, P. C., S. A. Rutledge, W. A. Petersen, and V. N. Bringi, 2001: *Journal of Applied Meteorology*, 40, 1347-1366.

Ryzhkov, A. V., T. J. Schuur, D. W. Burgess, P. L. Heinselman, S. E. Giangrande, and D. S. Zrnić, 2005: The joint polarization experiment: Polarimetric Rainfall measurements and hydrometeor classification. *Bull. Amer. Meteor. Soc.*, 86, 809-824.

----, D. Hudak, J. Scott, 2006: A new polarimetric scheme for attenuation

correction at C band Preprints, *Fourth European Conf. on Radar in Meteorology and Hydrology (ERAD 2006)*, Barcelona, Spain, 29-32.

----, D. S. Zrnić, P. Zhang, J. Krause, H. S. Park, D. Hudak, J. Young, J. L. Alford, M. Knight, and J. W. Conway, 2007: Comparison of Polarimetric Algorithms for Hydrometeor classification at S and C band. Preprints, *33rd AMS Conf. on Radar Meteorology*, Cairns, Queensland. http://ams.confex.com/ams/33Radar/techprogram/paper_123109.htm

----, P. Zhang, D. Hudak, J. L. Alford, M. Knight, and J. W. Conway, 2007: Validation of Polarimetric methods for attenuation correction at C band. Preprints, *33rd AMS Conf. on Radar Meteorology*, Cairns, Queensland. http://ams.confex.com/ams/33Radar/techprogram/paper_123122.htm